Quantitative Characterization of Tumoural Leakage Phenomena Using Dynamic Susceptibility Contrast Perfusion Imaging

Sriharish Vankayalapati
National Institute of Mental Health and Neurosciences: National Institute of Mental Health and Neuro Sciences

Karthik Kulanthaivelu
National Institute of Mental Health and Neurosciences: National Institute of Mental Health and Neuro Sciences

Vivek Lanka
National Institute of Mental Health and Neurosciences: National Institute of Mental Health and Neuro Sciences https://orcid.org/0000-0003-4323-1581

Dhritiman Chakrabarti
National Institute of Mental Health and Neurosciences: National Institute of Mental Health and Neuro Sciences

Jitender Saini
National Institute of Mental Health and Neurosciences: National Institute of Mental Health and Neuro Sciences

Maya Bhat
National Institute of Mental Health and Neurosciences: National Institute of Mental Health and Neuro Sciences

Chandrajit Prasad (chandrajitt2@gmail.com)
National Institute of Mental Health and Neurosciences: National Institute of Mental Health and Neuro Sciences

Hima Pendharkar
National Institute of Mental Health and Neurosciences: National Institute of Mental Health and Neuro Sciences

Abhishek Kotwal
National Institute of Mental Health and Neurosciences: National Institute of Mental Health and Neuro Sciences

Rajiv Mangla
Upstate University Hospital, New York

Kshitij Mankad
Great Ormond St Hosp Children: Great Ormond Street Hospital For Children NHS Foundation Trust

Nandeesh BN
National Institute of Mental Health and Neurosciences: National Institute of Mental Health and Neuro Sciences
Shilpa Rao
National Institute of Mental Health and Neurosciences: National Institute of Mental Health and Neuro Sciences
Dwarakanath Srinivas
National Institute of Mental Health and Neurosciences: National Institute of Mental Health and Neuro Sciences

---

Research Article

Keywords: Microvascular leakiness, blood brain barrier imaging, CNS Tumours, K2, DSC perfusion

Posted Date: February 25th, 2021

DOI: https://doi.org/10.21203/rs.3.rs-255428/v1

Quantitative Characterization of Tumoural Leakage Phenomena Using Dynamic Susceptibility Contrast Perfusion Imaging

Authors

Sriharish Vankayalapati [a], Karthik Kulanthaivelu [a], Vivek Lanka [a], Dhritiman Chakrabarti [b], Jitender Saini [a], Maya Bhat [a], Chandrajit Prasad [a], Hima Pendharkar [a], Abhishek Kotwal [a], Rajiv Mangla [c], Kshitij Mankad [d], Nandeesh BN [e], Shilpa Rao [e], Dwarakanath Srinivas [f].

[a] Department of Neuroimaging and Interventional Radiology, National Institute of Mental Health and Neurosciences, Bengaluru-560029, Karnataka, India.

[b] Department of Neuroanaesthesia and critical care, National Institute of Mental Health and Neurosciences, Bengaluru-560029, Karnataka, India

[c] Dept of Radiology, Upstate University Hospital , Newyork-13210, USA.

[d] Great Ormond Street Hospital, University College London Hospital.

[e] Department of Neuropathology, National Institute of Mental Health and Neurosciences, Bengaluru-560029, Karnataka, India

[f] Department of Neurosurgery, National Institute of Mental Health and Neurosciences, Bengaluru-560029, Karnataka, India

Corresponding author

Dr. Chandrajit Prasad, M.D., D.M.

Professor,

Department of Neuroimaging and Interventional Radiology,

National Institute of Mental Health and Neurosciences,

Bengaluru-Karnataka, India.560029

Email: chandrajitt2@gmail.com

Phone: +919489606741

ORCID: 0000-0001-6944-0926

Authors and Affiliations:

- Dr. Sriharish Vankayalapati, DNB.

  Senior resident,

  Department of Neuro Imaging Interventional Radiology,

  National Institute of Mental Health and Neuro Sciences,

  Bengaluru, Karnataka, India. 560029.

  Email: sriharish561@gmail.com.

  Phone: +919494869023

  ORCID: 0000-0001-5294-3324

- Dr Karthik Kulanthaivelu, M.D., D.M., F.R.C.R.

  Assistant Professor,

  Department of Neuroimaging and Interventional Radiology,

  National Institute of Mental Health and Neurosciences, Bengaluru,

  Karnataka, India 560029,

  Email: pammalkk@gmail.com.

  Phone: +918872723355

  ORCID: 0000-0002-1585-8769

- Dr. Vivek Lanka, M.D.

  Senior resident,

  Department of Neuro Imaging Interventional Radiology,

  National Institute of Mental Health and Neuro Sciences,

  Bengaluru, Karnataka, India. 560029.

  Email: lanka.vivek@gmail.com

  Phone: +919968511464

  ORCID: 0000-0003-4323-1581

- Dr. Dhritiman Chakrabarti, M.D., D.M.

  Assistant Professor, Department of Anaesthesia and neurocritical care,

  National Institute of Mental Health and Neurosciences, Bengaluru,

  Karnataka, India 560029.

  Email: dhritiman.ch@gmail.com

  Phone: +918197781240

  ORCID: 0000-0003-4804-5403

- Dr. Jitender saini, M.D., D.M.

  Professor,

  Department of Neuro Imaging and Interventional Radiology,

  National Institute of Mental Health and Neurosciences, Bengaluru,

  Karnataka, India 560029.

  Email: jsaini76@gmail.com

  Phone: +919980584819

  ORCID: 0000-0002-5218-0264

- Dr. Maya D Bhat, M.D., D.M.

  Additional Professor,

  Department of Neuro Imaging and Interventional Radiology,

  National Institute of Mental Health and Neurosciences, Bengaluru,

  Karnataka, India 560029.

  Email: mayabhat05@yahoo.co.in

  Phone: +919632688563

  ORCID: 0000-0003-3894-2071

- Dr. Chandrajit Prasad, M.D., D.M.

  Professor,

Department of Neuroimaging and Interventional Radiology,

National Institute of Mental Health and Neurosciences,

Bengaluru-Karnataka, India.560029

Email: chandrajitt2@gmail.com

Phone: +919489606741

ORCID: 0000-0001-6944-0926

- Dr. Hima Pendharkar, D.N.B., D.M.

  Professor

  Department of Neuroimaging and Interventional Radiology,

  National Institute of Mental Health and Neurosciences, Bengaluru-560029,

  Karnataka, India

  E-mail: himasp2@gmail.com

  Phone: +919663608548

  ORCID: 0000-0002-8711-7708

- Dr. Abhishek Kotwal, M.D.

  Senior resident, Department of Neuro Imaging and Interventional Radiology,

  National Institute of Mental Health and Neuro Sciences,

  Bengaluru, Karnataka, India. 560029.

  Email: abhishekkotwal2009@gmail.com

  Phone: +919315227524

  ORCID: 0000-0003-4308-1704

- Dr. Rajiv Mangla ,M.D.

  Associate Professor of radiology,

  Upstate University Hospital

  New York-13210, USA.

E-mail: manglar@ypstate.edu

Phone: +5858511302

- Dr. Kshitij Mankad MRCP, FRCR, PG Dip Hospital & Healthcare Mgmt., Lean 6 Sigma (Black Belt)

  Clinical Lead for Paediatric Neuroradiology & Associate Professor

  Great Ormond Street Hospital, University College London Hospital

  Email: drmankad@googlemail.com

  Phone: +447861639010

  ORCID: 0000-0001-5979-9337

- Dr. Nandeesh BN, MD, DNB.

  Associate Professor, Department of Neuropathology,

  National Institute of Mental Health and Neurosciences,
  Bengaluru-560029, Karnataka, India
  Email: nandeeshbn@gmail.com
  Phone: +919886489386

- Dr. Shilpa Rao M.D, D.M.

  Assistant Professor, Department of Neuropathology,

  National Institute of Mental Health and Neurosciences,
  Bengaluru-560029, Karnataka, India
  Email: shilpagk.rao@gmail.com
  Phone: +918105175956

  ORCID: 0000-0003-3067-6557

- Dr. Dwarakanath Srinivas, M.S., M. Ch.

  Professor, Department of Neurosurgery,
  National Institute of Mental Health and Neurosciences,
  Bengaluru-560029, Karnataka, India
  Email: dwarakaneuro@yahoo.com
  Phone: +919341268629

ORCID: 0000-0001-7330-0627

Abstract:

Purpose:

Microvascular Leakiness varies between tumours. Extravascular leakage, hitherto the Achilles heel of Dynamic-Susceptibility-Contrast-Perfusion-Weighted-Imaging (DSC-PWI), has lately been quantified by leakage coefficient "K2". To evaluate K2's diagnostic potential for differentiation of PCNSL, GBM and Mets and assess its relationships with other DSC-PWI metrics.

Methods:

Retrospective analysis of T2*-weighted DSC-PWI of PCNSL, Mets (n=10 each)and GBM n=16) was performed using a "Leakage Correction" model to generate K2 , uncorrected relative CBV (rCBVucor) and corrected rCBV (rCBVcor). Peak Signal Recovery (PSR) was calculated. Group-level statistical comparisons was made.

Results:

All PCNSL showed high-magnitude-positive K2 value with mean [SD] 846.1[462] while Mets showed high-magnitude-negative K2 value with mean [SD] -754[546]. In contrast, GBM showed varied values (overall with lower magnitude and positive) of K2 with mean [SD] 391.9[294.1]. The intergroup differences in K2 were statistically different (P 0.000). Lesion K2 (magnitude) exhibited a significant strong positive correlation with the magnitude of CBV correction (ρ 0.63) and with PSR (ρ 0.70).

Conclusion:

PCNSL had greater high-magnitude-positive-K2 compared with other tumour groups, while Mets were notable for a high-magnitude-negative-K2. K2 parameter obtained from T2*-weighted DSC technique characterizes and quantifies microvascular leakage of contrast and thus provides an alternative means of measuring permeability in tumours. K2 quantification adds adjunctive value to pre-operative discrimination of intra-axial neoplasms. Given the widespread acceptance that DSC-PWI has, K2 holds promise as an attractive alternative to (the methodologically challenging) DCE-PWI-derived permeability metric, K^{trans}.

Keywords: Microvascular leakiness, blood brain barrier imaging, CNS Tumours, K2, DSC perfusion.

Declarations:

Funding – No funding was received for this study.

Conflicts of Interest/Competing Interests – The authors have no conflicts of interest to declare that are relevant to the content of this article.

Availability of data and material – The datasets generated during and/or analysed during the current study are available from the corresponding author on reasonable request.

Code availability – Not applicable.

Authors' contributions – Conceptualization: Karthik Kulanthaivelu, Chandrajit Prasad, Maya Bhat; Methodology: Sriharish Vankayalapati, Vivek Lanka, Dhritiman Chakrabarti, Abhishek Kotwal, Nandeesh BN, Shilpa Rao; Writing - original draft preparation: Sriharish Vankayalapati, Karthik Kulanthaivelu, Vivek Lanka; Writing - review and editing: Jitender Saini, Chandrajit Prasad, Maya Bhat, Hima Pendharkar, Rajiv Mangla, Kshitij Mankad, Dwarakanath Srinivas.

Ethics approval: As our work was a retrospective study, informed consent was waivered off by our Institional Ethics Committee.

Consent to participate: Not applicable.

Consent for publication: Not applicable.

Introduction:

Pre-treatment definition of malignant intra-axial neoplasms using conventional/advanced MR imaging is challenging. A frequently encountered conundrum is differentiation among primary central nervous system lymphomas (PCNSL) glioblastomas (GBM) and metastases (Mets), which may appear similar on conventional MR sequences as solitary, avidly enhancing brain tumours with brisk peri-tumoural edema. Needless to say, their management strategies deviate: Treatment of GBM and Mets revolves around surgical resection, radiotherapy, and chemotherapy, while PCNSL are primarily subjected to chemotherapy[1].

Perfusion weighted imaging (PWI) helps uncover information on microvascular physiology and pathology. Among the PWI techniques, dynamic susceptibility contrast (DSC-PWI) imaging has found wide acceptance. DSC-PWI, is based on dynamic measurement of the drop of MR signal on a T2*-weighted sequence during the first pass of bolus of a Gadolinium-based contrast agent (GBCA)[2]. As regards tumours, DSC-PWI estimates their microvascular density from relative cerebral blood volume (rCBV)[3].

Early literature in DSC-PWI emphasized on rCBV for characterizing and differentiating tumour groups[4, 5]. However, other perfusion parameters derived from signal intensity-time (SI-T) curves, viz., peak height or percentage of signal recovery (PSR), could be better suited for tumour differentiation, compared to rCBV [6, 7].

Microvascular permeability ("leakiness") (MVL) has lately received much attention in the characterisation of tumour biology. Histologically, the microvascular structure of GBM, Mets, and PCNSL is different; so is their MVL[8–10]. While MVL has been the center stage and forte of Dynamic Contrast-Enhanced Perfusion Imaging (DCE-PWI), it has been the Achilles heel of DSC-PWI in most of the literature. DCE-MRI has its challenges in the

standardization of assumptions for pharmacokinetic modelling of leakage[2]. From a DSC-PWI standpoint, MVL/blood-brain-barrier (BBB) leakiness may be indirectly inferred from a recently described and modified leakage coefficient, termed “K2” to help understand the differences in BBB integrity among the different tumours[11, 12]. Literature discussing MVL (from a DSC-PWI standpoint) in grading gliomas[13] or differentiating tumours is sparse[14]. We hypothesized that this DSC-PWI derived metric of MVL ("K2") is different among PCNSL, GBM, and Mets. In this study, we intend to evaluate the performance of K2 in the differentiation of PCNSL, GBM, and Mets and assess its association with other DSC-PWI derived perfusion parameters.

Material and Methods:

Study Population:

The study is retrospective-observational. All patients with intra-axial space-occupying-lesions evaluated with DSC-PWI in our institution between January 2019 and March 2020 were considered. Cases whose histopathology was PCNSL, GBM, or Mets were included in the final analysis.

Data acquisition:

Examinations were performed on 3T MR (Philips Ingenia; Philips Healthcare, Netherlands) using a 32-channel Head/Neck/Spine coil. A standard MR examination was initially carried out, including axial T1-W, T2-W (axial, coronal and sagittal), Fluid attenuated inversion recovery, Diffusion-Weighted Imaging, and Susceptibility Weighted Imaging. DSC-PWI was then acquired followed by post-contrast 3D T1-weighted imaging.

Perfusion weighted imaging (PWI):

DSC-PWI was executed using an echo-planar T2*-weighted gradient-echo sequence (TR=1605ms/TE=40 ms/Flip angle=75degree/Field-Of-View=10 cm/ Matrix=96 x 94/Bandwidth=2163Hz per pixel/Voxel size=2.3x2.3x4mm/Slice thickness= 4mm/Excitations-1). After ten baseline acquisitions, a bolus of 0.1ml/kg of 0.5 mmol/l of gadoteric acid contrast agent (Clariscan, GE Health care, Princeton, NJ) was administered via an 18/20G cannula intravenously using an automatic pressure injector (Spectris Solaris, Medrad, Pittsburgh, PA, USA) at a rate of 5ml/sec, followed by a saline chase of 20 ml at a rate of 5ml/sec. The acquisition lasted 1 min 6 sec.

Image post-processing of perfusion-weighted imaging:

The DSC-PWI data was post-processed offline using Philips Intellispace software (version10.1.89).

The MR-NeuroPerfusion module in the software package has four schemes for data analysis - 1. Model-free; 2. Gamma Variate; 3. Manual AIF; 4. Leakage Correction.

The latter two methods were used to obtain the various perfusion metrics in this study:

1. The model with a manual prescription of AIF, which is then deconvoluted from the tissue concentration-time curve for estimating a tissue residue function[15], in-turn estimating the rCBV – hereby referred to as ‘rCBV from manual AIF’.

2. A leakage correction model with its mathematical basis as proposed by Weisskoff et al. and later refitted by Donahue et al. and Boxerman et al.[16]

The leakage correction scheme of analysis was of primary interest in this study[16]. Computed metrics included K2 (a coefficient of leakage), uncorrected rCBV (rCBVucor), and corrected rCBV (rCBVcor). In areas with contrast-agent leakage, a complex interplay of competing T1 shortening and T2* shortening effects of the leaked GBCA, influences the shape of the relaxivity–time curve. Linear fitting was used to estimate a 'corrected' relaxivity-time curve and a leakage correction term was obtained. From this, a first-order estimate of the vascular permeability (K2) was generated[16]. rCBVucor and rCBVcor were calculated from the uncorrected and the corrected relaxivity-time curves respectively.

Multiparametric maps, thus obtained, were co-registered with post-contrast 3D T1-weighted images. Regions of interest (ROI), were positioned on solid tumour components, ensuring to include areas with the highest rCBVcor on visual inspection (ROIs initially placed using rCBVcor maps as reference, were copied to the other parametric maps to maintain uniformity). Caution was taken to avoid large vessels, hemorrhage and necrosis contaminating the ROIs. ROIs' size was kept constant at 40-50 mm^2.

ROI derived T2*-weighted SI-T curves, were used to calculate PSR as described by Cha et al.[7]

$$PSR = 100 \times \frac{(S_i - S_{min})}{(S_0 - S_{min})}$$

S_i – post-contrast T2*-weighted signal intensity at the end of the first pass; S_0 – pre-contrast T2*-weighted signal intensity at baseline; S_{min} – T2*-weighted signal intensity at the trough of the first pass.

The various derived perfusion metrics, were then normalised to corresponding values from contralateral hemispheric normal-appearing white matter (NAWM) in order to achieve inter/intrasubject comparability.

Statistical analysis:

Data was collated offline on Microsoft Excel (ver.15.0.4) and statistical analysis was conducted using R software (Ver.3.5.2). The parameters evaluated were rCBVucor (rCBV uncorrected), rCBVcor (rCBVcorrected) K2, PSR, rCBV correction magnitude (rCBVcor-rCBVucor), rCBV ratio [rCBV (lesion)/ rCBV(NAWM)], K2 difference [K2 diff = K2 difference between NAWM and lesion ROI]. The descriptive data are presented as mean ±SD. Between-group comparison was performed using the Kruskal Wallis test for > 2 groups and Mann-Whitney-U test for 2 group comparisons. Spearman's method was used for between-parameter correlations. Parameter cut-offs for distinguishing tumour types were determined by Receiver Operating Characteristic Curve (ROC) analysis. $p<0.05$ was considered significant.

Results:

Anonymized pre-operative MR imaging data from 36 patients was included in the final analysis (PCNSL, Mets n=10 each; GBM n=16). The groups had comparable demographics (age and gender).

The lesions (supratentorial-33; infratentorial-3) appeared on conventional imaging as enhancing, well-delineated lesions with moderate-severe perilesional edema. Three metastases were from lung, two from thyroid, one-each from leukemia, kidney, and colon, while two had unknown primary.

The key perfusion metrics of the three tumour groups are tabulated in Table 1, and those which attained statistical significance for tumour group differentiation are highlighted in Table 2. A pictorial summary of the perfusion metric maps is presented in Fig 1-3. All PCNSL showed high-magnitude-positive K2 values with mean[SD] 846.1[462] while Mets showed high-magnitude-negative K2 values with mean[SD] -754[546]. In contrast, GBM showed varied values (overall positive with lower magnitude) of K2 with mean[SD] 391.9[294.1]. The intergroup differences in K2 were statistically different (P 0.000).

The mean rCBVucor ratio (normalized) for PCNSL, GBM and Mets were 1.57, 4.5, and 7.79 respectively, while rCBVcor ratio (normalized) were 4.3, 4.7, and 5.27 respectively. Compared to Mets/ GBMs, PCNSLs had a significantly lower normalized rCBVucor ratio. Intergroup differences in uncorrected rCBV values (rCBVucor) was significant (P 0.000). Interestingly, the direction of correction of rCBV values tended towards an increase in PCNSL and GBM (Correction magnitude PCNSL > GBM), while it tended towards a reduction in Mets. The magnitude and direction of the correction of rCBV were +138, +60, and –109.4 for the PCNSL, GBM, and Mets groups, respectively (P- 0.001). No significant intergroup difference was identified in the rCBVcor values after the correction for leakage (P- 0.299). The mean[SD] of PSR was 104.3[17.5], 70.9[14.1], and 56.5[12.4] for the PCNSL, GBM, and Mets groups, respectively. The intergroup difference in the PSR was statistically significant (P 0.000). Correlation among the perfusion metrics across the groups is represented as a correlogram (eFig 1; Online Resource 1). Lesion K2 (magnitude) exhibited a significant strong positive correlation with the magnitude of CBV correction (ρ 0.63) and with PSR (ρ 0.70). A significant negative correlation with MTT (derived from a manual AIF analysis) was noted (ρ-0.67). The rCBVuncor derived in leakage correction exhibited a significant positive correlation with rCBV obtained from manual AIF (ρ 0.86).

ROC analysis of various DSC-PWI metrics is depicted in eFig 2 (Online Resource 1) and eTable 1 (Online Resource 1). ROC analysis of the evaluated parameters showed the largest area under the curve (AUC) for PSR to differentiate PCNSLs from GBM. AUC was higher for K2 compared to PSR to discriminate PCNSLs vs. Mets, and GBM vs. Mets. K2 thresholds for intergroup differentiation are summarized in eTable 2 (Online Resource 1).

Discussion:

A summary of the key observations (centered on K2) in our study is: PCNSL have high-magnitude-positive-K2 compared to other tumour groups: GBMs – lower-magnitude-positive-K2; Mets – high-magnitude-negative-K2. Our results underscore the value of K2 as a quantitative diagnostic metric and a potential surrogate of vascular permeability, a seldom discussed attribute in DSC-PWI parlance.

The most commonly used DSC-PWI metric in neuro-oncology is rCBV. It has been used for glioma grading[17], and differentiation of glioblastoma, metastasis, and lymphoma[1, 5, 18]. rCBV is a surrogate of tumour vascularity on the assumption of BBB integrity[19]. However, BBB disruption, almost invariable in neoplasms, allows GBCA extravasation[17].

Quests for better accuracy in CBV measurement, inspired a mathematic model for leakage correction[16]. With reference to high-grade gliomas, Weiskoff et al.,[16] showed that the corrected-CBV had a better correlation with tumour grade than the uncorrected-CBV. This method linearly fits measured R2*(t) to two constant functions derived from the average relaxation rate of non-enhancing tissue. One of the constants is a permeability-weighted coefficient "K2", proportional to leakage (PS, where PS is the product of permeability and surface area)[16].

$$K2 = \frac{TR}{TE} \cdot \frac{e^{-TR \cdot R_{10}}}{1 - e^{-TR \cdot R_{10}}} \cdot r_1 \cdot k \cdot PS$$

Preliminary work demonstrated significant differences in K2 among gliomas of different grades[13] and between PCNSL and glioma[14], a reflection of their innate differences in vascular permeability.

The assumptions underlying the Weiskoff's model however limit its validity to conditions where all of the leakage manifests as T1 effects. Liu et al,[11], demonstrated that leakage in-fact presents as a complex interplay of competing T1 and T2* effects. GBCA induced T1 relaxivity changes are microscale effects, that stem from T1 shortening of protons adjacent to the GBCA molecule. In contrast, T2* relaxivity changes result from superposition of meso-scale field perturbations induced by susceptibility gradients across tissue compartment interfaces[20]. Hence, a homogeneous distribution of the leaked interstitial GBCA is likely to exhibit T1 dominant signal behaviour, while a compartmentalised/heterogeneous distribution, favours T2* effects.[20]

The positive-negative dichotomy to the interpretation of K2 values that we underscore among PCNSL, GBM, and Mets borrows from the work of Liu et al.[11]

$$K2 = \frac{PS}{Vp}\left(\frac{TR}{TE} \cdot \frac{e^{-TR \cdot R_{10}}}{1 - e^{-TR \cdot R_{10}}} \cdot \frac{r_1}{r_2} - 1\right)$$

The information portrayed by K2 is two-fold – its magnitude estimates the degree of MVL; while its sign represents the dominant signal behaviour of the leaked GBCA (T1 dominant effects – positive K2; T2* dominant effects – negative K2).

Microvascular and interstitial architectural characteristics show considerable differences in GBM, Mets, and PCNSL[21]. Ultrastructural changes of capillary endothelial fenestrations,

and intermittent absence of endothelium in PCNSL[22] are likely to account for its increased vascular permeability and GBCA leakage[14],[23]. The unique tumour cell distribution in PCNSL (multiple thick uniform layers around the host vessels[24]) forges a spatially homogeneous interstitium and thus, the leaked GBCA. This homogeneity weakens T2* shortening, unmasking the T1 effect. The high-magnitude-positive K2 values featured in our cohort of PCNSL, mirror these T1 dominant leakage effects.

As regards Mets, Long et al.,[25] in their electron microscopic examination study, pointed to a resemblance of the capillary architecture of intra-axial metastatic lesions, to that of their tissues of origin, as against capillaries of native brain tissue (implying significantly increased MVL). Interestingly, Mets also show higher orders of cellular organisation (into acini/tubules/spindles depending on the tissue of origin)[26], forging heterogeneity/mesoscale compartmentalisation within the interstitium, and thus, the egressed GBCA. As a corollary, T2* shortening dominates, eclipsing the weak T1 effect. The high-magnitude-negative K2 values manifested in our cohort of Mets, reflect these T2* dominant leakage effects.

GBM capillaries are known for heterogeneity in their morphology. Rojiani and Dorovini-Zis[27] showed that the GBM microvasculature could retain some aspects of BBB architecture due to closely packed capillary buds that are lined by hyperplastic endothelial cells and partly invested by pericytes. This results in varying degree of permeability across GBM capillaries, ranging from near-normal to increased[27]. These features may factor in the observed heterogeneity and high variance in K2 values in the GBM group. We propose that this relatively attenuated BBB disruption in GBM, manifests as intermediate K2 values.

A positive correlation of K2 with PSR was noted in our study. Mangla et al. reported that the PSR was significantly higher in PCNSLs compared to GBM, and it differentiates PCNSLs from GBM and Mets better than rCBV[6]. PSR is perhaps another approach to

(semi)quantitate leakage phenomenon across tumours[6, 7, 28]. While a K2-PSR relationship appears theoretically plausible, our work (for the first time) has convincingly demonstrated the quantitative reciprocity of PSR with K2. In as much as PSR value can differentiate different tumour groups[6, 7, 28], we propose that K2 can differentiate PCNSL vs. GBM vs. Mets.

Capillary flow limitation may be another confound. Microvascular blood flow in GBM is often altered by abnormal tumour neo-vasculature comprising tortuous, defective channels, immature endothelium and/or thrombosis. Hence, the low GBCA leakage in GBM, may be a product of flow-limitation[29]. In contrast, PCNSLs exhibit near absence of neovascularization coupled with substantial disruption of the BBB[6]. These morphologic differences may make the GBCA leakage less flow-limited in PCNSLs compared with GBM and may account for our observation of significantly higher K2 values in PCNSLs than GBM.

We explore the possible homology of the DSC-derived leakage metric (K2) with its DCE-PWI derived counterpart (K^{trans}). Quite intuitively, a recent study found a positive linear correlation between K_2 and K^{trans} when comparing maximum whole-tumour values across patients[30]. Prior work has highlighted that the K^{trans} of PCNSL is usually higher than that of GBM and Mets[31] analogous to the K2 observations in our study. At least two earlier accounts, one each probing K2 differences between PCNSL Vs. GBM and GBM Vs. Mets[9, 14] have demonstrated observations similar to ours. To the best of our knowledge, this work is the first to illustrate the quantitative differences in the K2 leakage co-efficient between PCNSL and Mets. It is to be noted that the correlation between DCE-PWI-derived perfusion metric Vp (plasma volume fraction) and its DSC-PWI-derived analog, rCBV has been inconsistent across studies[32, 33].

As expected, K2 values showed a correlation with the CBV correction magnitude in our study. The (K2-driven) corrections to the rCBVuncor are polar in PCNSL and Mets. While it corrects systematic underestimations in PCNSL, in case of Mets, it is the overestimations, which are rectified. DSC literature describing perfusion in PCNSL vs. GBM vs. Mets has consistently emphasised lower perfusion (rCBVuncor ratios) in PCNSL[1, 5, 14, 18]. This hitherto claimed lower CBV in PCNSL ought to be interpreted in light of the uncorrected nature of those values. It is noteworthy that the leakage corrected rCBV ratios calculated in this study weren't significantly different between tumour types. This observation is not without precedence. Lu et al., using DCE-PWI, noted no difference in the Vp (DCE analog of rCBV) between PCNSL and GBM/Mets[31]. Elsewhere, conflicting K^{trans} and Vp (no significant difference and reduced, respectively) trends have been described in PCNSL vs. GBM[10, 34].

K2 has multifactorial determinants beyond tumour histology. Besides permeability and surface area, K2 may be modulated by many factors, including but not limited to, T2* and T1 relaxivity, longitudinal recovery rate, TR, TE, and flip angle[17]. A one-dimensional leakage simulation study performed by Quarles et al[35] demonstrated that when T1 shortening effects were removed, such as with the use of a dual-/multi-echo sequence, the measured transverse relaxation-rate-time course overestimated the true transverse relaxation–rate-time course. Therefore, the CBV was likely to be overestimated. When T1 shortening effects dominated (when the high flip angle and short repetition time were used), the measured transverse relaxation-rate-time course underestimated the true transverse relaxation-rate-time course; thus, the CBV would be underestimated.[36] K2 may not correlate linearly with the permeability, due to a complex relationship between GBCA concentration in tissue and the measured change in signal intensity, but may show a positive correlation with the K^{trans} at

high flip angles[16]. DSC Perfusion data acquired with a uniform flip angle of 75 degrees in our study allowed a comparison of K2 between our tumour groups.

Leakage correction model used in our study assumes similar bolus arrival time and MTT in tumour and normal-appearing tissue[37]. To mitigate this problem, an alternative MTT-insensitive correction method has been proposed by Quarles et al.[35] which calculates the tissue-specific residue function R(t), to provide better estimates of tumour permeability[15].

Our study is limited by its retrospective nature and a lack of direct correlation between perfusion parameters and immunohistochemical/histomorphological markers of microvessel density and endothelial ultrastructure. No immunohistochemical information on Vascular Endothelial Growth Factor (VEGF) expression was available. While many factors viz., vascular surface area; vascular permeability; blood flow; and hydrostatic, interstitial, and osmotic gradients across the endothelium may summate and influence K2, the quantitative/qualitative contributions of each factor couldn't be measured in vivo. We have not used any of the recently surfaced DSC-PWI techniques with pre-load correction (pre-load GBCA was not administered) and/or dual-echo acquisition[35]. Our exploration of the K2-K^{trans} relationship has largely been speculative, as inferred from literature as no DCE-PWI was performed in this series.

In conclusion, K2 leakage coefficient obtained from DSC-PWI, characterizes and quantifies microvascular contrast leakage and thus provides an alternative means measure of permeability in tumours. PCNSL has high-magnitude-positive-K2 compared with other tumour groups, while Mets were notable for a high-magnitude-negative-K2. The inter-relationship of K2 and PSR has been illustrated. K2 quantification adds adjunctive value to pre-operative discrimination of intra-axial neoplasms. Given the widespread acceptance of

DSC-PWI, K2 holds promise as an attractive alternative to (the methodologically challenging) DCE-PWI-derived permeability metrics.

Acknowledgements: none.

REFERENCES:

1. Liao W, Liu Y, Wang X, et al (2009) Differentiation of Primary Central Nervous System Lymphoma and High-Grade Glioma with Dynamic Susceptibility Contrast-Enhanced Perfusion Magnetic Resonance Imaging. Acta Radiol 50:217–225. https://doi.org/10.1080/02841850802616752

2. Essig M, Shiroishi MS, Nguyen TB, et al (2013) Perfusion MRI: The Five Most Frequently Asked Technical Questions. Am J Roentgenol 200:24–34. https://doi.org/10.2214/AJR.12.9543

3. Rosen BR, Belliveau JW, Vevea JM, Brady TJ (1990) Perfusion imaging with NMR contrast agents. Magn Reson Med 14:249–265. https://doi.org/10.1002/mrm.1910140211

4. Makino K, Hirai T, Nakamura H, et al (2018) Differentiating Between Primary Central Nervous System Lymphomas and Glioblastomas: Combined Use of Perfusion-Weighted and Diffusion-Weighted Magnetic Resonance Imaging. World Neurosurg 112:e1–e6. https://doi.org/10.1016/j.wneu.2017.10.141

5. Neska-Matuszewska M, Bladowska J, Sąsiadek M, Zimny A (2018) Differentiation of glioblastoma multiforme, metastases and primary central nervous system lymphomas using multiparametric perfusion and diffusion MR imaging of a tumor core and a peritumoral zone—Searching for a practical approach. PLOS ONE 13:e0191341. https://doi.org/10.1371/journal.pone.0191341

6. Mangla R, Kolar B, Zhu T, et al (2011) Percentage signal recovery derived from MR dynamic susceptibility contrast imaging is useful to differentiate common enhancing malignant lesions of the brain. AJNR Am J Neuroradiol 32:1004–1010. https://doi.org/10.3174/ajnr.A2441

7. Cha S, Lupo JM, Chen M-H, et al (2007) Differentiation of Glioblastoma Multiforme and Single Brain Metastasis by Peak Height and Percentage of Signal Intensity Recovery Derived from Dynamic Susceptibility-Weighted Contrast-Enhanced Perfusion MR Imaging. Am J Neuroradiol 28:1078–1084. https://doi.org/10.3174/ajnr.A0484

8. Ma JH, Kim HS, Rim N-J, et al (2010) Differentiation among glioblastoma multiforme, solitary metastatic tumor, and lymphoma using whole-tumor histogram analysis of the normalized cerebral blood volume in enhancing and perienhancing lesions. AJNR Am J Neuroradiol 31:1699–1706. https://doi.org/10.3174/ajnr.A2161

9. Server A, Orheim TED, Graff BA, et al (2011) Diagnostic examination performance by using microvascular leakage, cerebral blood volume, and blood flow derived from 3-T dynamic susceptibility-weighted contrast-enhanced perfusion MR imaging in the

differentiation of glioblastoma multiforme and brain metastasis. Neuroradiology 53:319–330. https://doi.org/10.1007/s00234-010-0740-3

10. Kickingereder P, Sahm F, Wiestler B, et al (2014) Evaluation of microvascular permeability with dynamic contrast-enhanced MRI for the differentiation of primary CNS lymphoma and glioblastoma: radiologic-pathologic correlation. AJNR Am J Neuroradiol 35:1503–1508. https://doi.org/10.3174/ajnr.A3915

11. Liu H-L, Wu Y-Y, Yang W-S, et al (2011) Is Weisskoff model valid for the correction of contrast agent extravasation with combined and effects in dynamic susceptibility contrast MRI? Med Phys 38:802–809. https://doi.org/10.1118/1.3534197

12. Boxerman JL, Prah DE, Paulson ES, et al (2012) The Role of Preload and Leakage Correction in Gadolinium-Based Cerebral Blood Volume Estimation Determined by Comparison with MION as a Criterion Standard. AJNR Am J Neuroradiol 33:1081–1087. https://doi.org/10.3174/ajnr.A2934

13. Server A, Graff BA, Orheim TED, et al (2011) Measurements of diagnostic examination performance and correlation analysis using microvascular leakage, cerebral blood volume, and blood flow derived from 3T dynamic susceptibility-weighted contrast-enhanced perfusion MR imaging in glial tumor grading. Neuroradiology 53:435–447. https://doi.org/10.1007/s00234-010-0770-x

14. Toh CH, Wei K-C, Chang C-N, et al (2013) Differentiation of Primary Central Nervous System Lymphomas and Glioblastomas: Comparisons of Diagnostic Performance of Dynamic Susceptibility Contrast-Enhanced Perfusion MR Imaging without and with Contrast-Leakage Correction. Am J Neuroradiol 34:1145–1149. https://doi.org/10.3174/ajnr.A3383

15. Bjornerud A, Sorensen AG, Mouridsen K, Emblem KE (2011) T1- and T2*-dominant extravasation correction in DSC-MRI: part I--theoretical considerations and implications for assessment of tumor hemodynamic properties. J Cereb Blood Flow Metab Off J Int Soc Cereb Blood Flow Metab 31:2041–2053. https://doi.org/10.1038/jcbfm.2011.52

16. Boxerman JL, Schmainda KM, Weisskoff RM (2006) Relative cerebral blood volume maps corrected for contrast agent extravasation significantly correlate with glioma tumor grade, whereas uncorrected maps do not. AJNR Am J Neuroradiol 27:859–867

17. Paulson ES, Schmainda KM (2008) Comparison of Dynamic Susceptibility-weighted Contrast-enhanced MR Methods: Recommendations for Measuring Relative Cerebral Blood Volume in Brain Tumors. Radiology 249:601–613. https://doi.org/10.1148/radiol.2492071659

18. Hartmann M, Heiland S, Harting I, et al (2003) Distinguishing of primary cerebral lymphoma from high-grade glioma with perfusion-weighted magnetic resonance imaging. Neurosci Lett 338:119–122. https://doi.org/10.1016/s0304-3940(02)01367-8

19. Zaharchuk G (2007) Theoretical Basis of Hemodynamic MR Imaging Techniques to Measure Cerebral Blood Volume, Cerebral Blood Flow, and Permeability. Am J Neuroradiol 28:1850–1858. https://doi.org/10.3174/ajnr.A0831

20. Koch T, Flemisch B, Helmig R, et al (2020) A multiscale subvoxel perfusion model to estimate diffusive capillary wall conductivity in multiple sclerosis lesions from perfusion MRI data. Int J Numer Methods Biomed Eng 36:e3298. https://doi.org/10.1002/cnm.3298

21. Wesseling P, Ruiter DJ, Burger PC (1997) Angiogenesis in brain tumors; pathobiological and clinical aspects. J Neurooncol 32:253–265. https://doi.org/10.1023/A:1005746320099

22. Molnár PP, O'Neill BP, Scheithauer BW, Groothuis DR (1999) The blood-brain barrier in primary CNS lymphomas: Ultrastructuralevidence of endothelial cell death. Neuro-Oncol 1:89–100. https://doi.org/10.1093/neuonc/1.2.89

23. Warnke PC, Timmer J, Ostertag CB, Kopitzki K (2005) Capillary physiology and drug delivery in central nervous system lymphomas. Ann Neurol 57:136–139. https://doi.org/10.1002/ana.20335

24. Sugita Y, Muta H, Ohshima K, et al (2016) Primary central nervous system lymphomas and related diseases: Pathological characteristics and discussion of the differential diagnosis. Neuropathology 36:313–324. https://doi.org/10.1111/neup.12276

25. Long DM (1979) Capillary ultrastructure in human metastatic brain tumors. J Neurosurg 51:53–58. https://doi.org/10.3171/jns.1979.51.1.0053

26. Pekmezci M, Perry A (2013) Neuropathology of brain metastases. Surg Neurol Int 4:S245–S255. https://doi.org/10.4103/2152-7806.111302

27. Rojiani AM, Dorovini-Zis K (1996) Glomeruloid vascular structures in glioblastoma multiforme: an immunohistochemical and ultrastructural study. J Neurosurg 85:1078–1084. https://doi.org/10.3171/jns.1996.85.6.1078

28. Law M, Cha S, Knopp EA, et al (2002) High-Grade Gliomas and Solitary Metastases: Differentiation by Using Perfusion and Proton Spectroscopic MR Imaging. Radiology 222:715–721. https://doi.org/10.1148/radiol.2223010558

29. Cha S (2006) Update on Brain Tumor Imaging: From Anatomy to Physiology. Am J Neuroradiol 27:475–487

30. Bonekamp D, Deike K, Wiestler B, et al (2015) Association of overall survival in patients with newly diagnosed glioblastoma with contrast-enhanced perfusion MRI: Comparison of intraindividually matched T1- and T2*-based bolus techniques. J Magn Reson Imaging 42:87–96. https://doi.org/10.1002/jmri.24756

31. Lu S, Gao Q, Yu J, et al (2016) Utility of dynamic contrast-enhanced magnetic resonance imaging for differentiating glioblastoma, primary central nervous system lymphoma and brain metastatic tumor. Eur J Radiol 85:1722–1727. https://doi.org/10.1016/j.ejrad.2016.07.005

32. Bazyar S, Ramalho J, Eldeniz C, et al (2016) Comparison of Cerebral Blood Volume and Plasma Volume in Untreated Intracranial Tumors. PLOS ONE 11:e0161807. https://doi.org/10.1371/journal.pone.0161807

33. Alcaide-Leon P, Pareto D, Martinez-Saez E, et al (2015) Pixel-by-Pixel Comparison of Volume Transfer Constant and Estimates of Cerebral Blood Volume from Dynamic Contrast-Enhanced and Dynamic Susceptibility Contrast-Enhanced MR Imaging in High-Grade Gliomas. Am J Neuroradiol 36:871–876. https://doi.org/10.3174/ajnr.A4231

34. Lin X, Lee M, Buck O, et al (2017) Diagnostic Accuracy of T1-Weighted Dynamic Contrast-Enhanced–MRI and DWI-ADC for Differentiation of Glioblastoma and Primary CNS Lymphoma. Am J Neuroradiol 38:485–491. https://doi.org/10.3174/ajnr.A5023

35. Quarles CC, Gochberg DF, Gore JC, Yankeelov TE (2009) A theoretical framework to model DSC-MRI data acquired in the presence of contrast agent extravasation. Phys Med Biol 54:5749–5766. https://doi.org/10.1088/0031-9155/54/19/006

36. Korfiatis P, Erickson B (2014) The basics of diffusion and perfusion imaging in brain tumors. Appl Radiol 43:22

37. Emblem KE, Bjornerud A, Mouridsen K, et al (2011) T1- and T2*-Dominant Extravasation Correction in DSC-MRI: Part II—Predicting Patient Outcome after a Single Dose of Cediranib in Recurrent Glioblastoma Patients. J Cereb Blood Flow Metab 31:2054–2064. https://doi.org/10.1038/jcbfm.2011.39

Figures legends:

Fig 1 A 60year male known case of carcinoma left upper lobe presented with late onset of headache. CT (a) and conventional MRI (b-f) axial images show a solid cystic lesion in the left parietal region with minimal perilesional edema. The solid component is heterogeneously hyperdense on CT (a) and is iso-hyperintense on T2Wimage (b) with subtle foci of blooming on SWI (c), partial restricted diffusion (d,e) and moderate post-contrast enhancement (f). DSC Perfusion (g) evaluated with the "Leakage correction" model is shown with corresponding multiparametric maps (h-j). rCBVuncor (h), rCBVcor (i), K2map(j), Time-signal intensity curve(k) and perfusion metrics (l) reveal a negative high K2 value and about 65.7% mean signal-intensity recovery. The lesion proved to be metastasis on histopathology.

Fig 2 A 58year male with altered sensorium. CT (a) and conventional MRI (b-f) axial images show a solid lesion in the left anterior caudate adjoining the periventricular white matter in the left frontal lobe with moderate perilesional edema. The lesion is hyperdense on CT (a)

and hyperintense on T2Wimage (b) with patchy areas of internal blooming on SWI (c), patchily restricted diffusion (d, e) and homogenous dense post-contrast enhancement (f). DSC Perfusion (g) evaluated with the "Leakage correction" model is shown with corresponding multiparametric maps (h-j). rCBVuncor (h), rCBVcor (i), K2map(j), Time-signal intensity curve (k) and perfusion metrics (l) reveal a positive high K2 value and about 124% mean signal-intensity recovery. Note the clear overshoot from the baseline. The lesion proved to be a B cell lymphoma on histopathology.

Fig 3 A 67year male with left hemiplegia. CT (a) and conventional MRI (b-f) axial images show a solid lesion in the right parietal region with moderate perilesional edema. The lesion is hyperdense on CT (a) and is hyperintense on T2Wimage (b) with subtle foci of blooming on SWI (c), mild homogeneous restriction of diffusion (d, e) and mild homogenous post-contrast enhancement (f). DSC Perfusion (g) evaluated with the "Leakage correction" model is shown with corresponding multiparametric maps (h-j). rCBVuncor (h), rCBVcor (i), K2map(j), Time-signal intensity curve(k) and perfusion metrics (l) reveal a negative K2 value and about 80% mean signal-intensity recovery. The lesion proved to be a glioblastoma on histopathology.

Figures

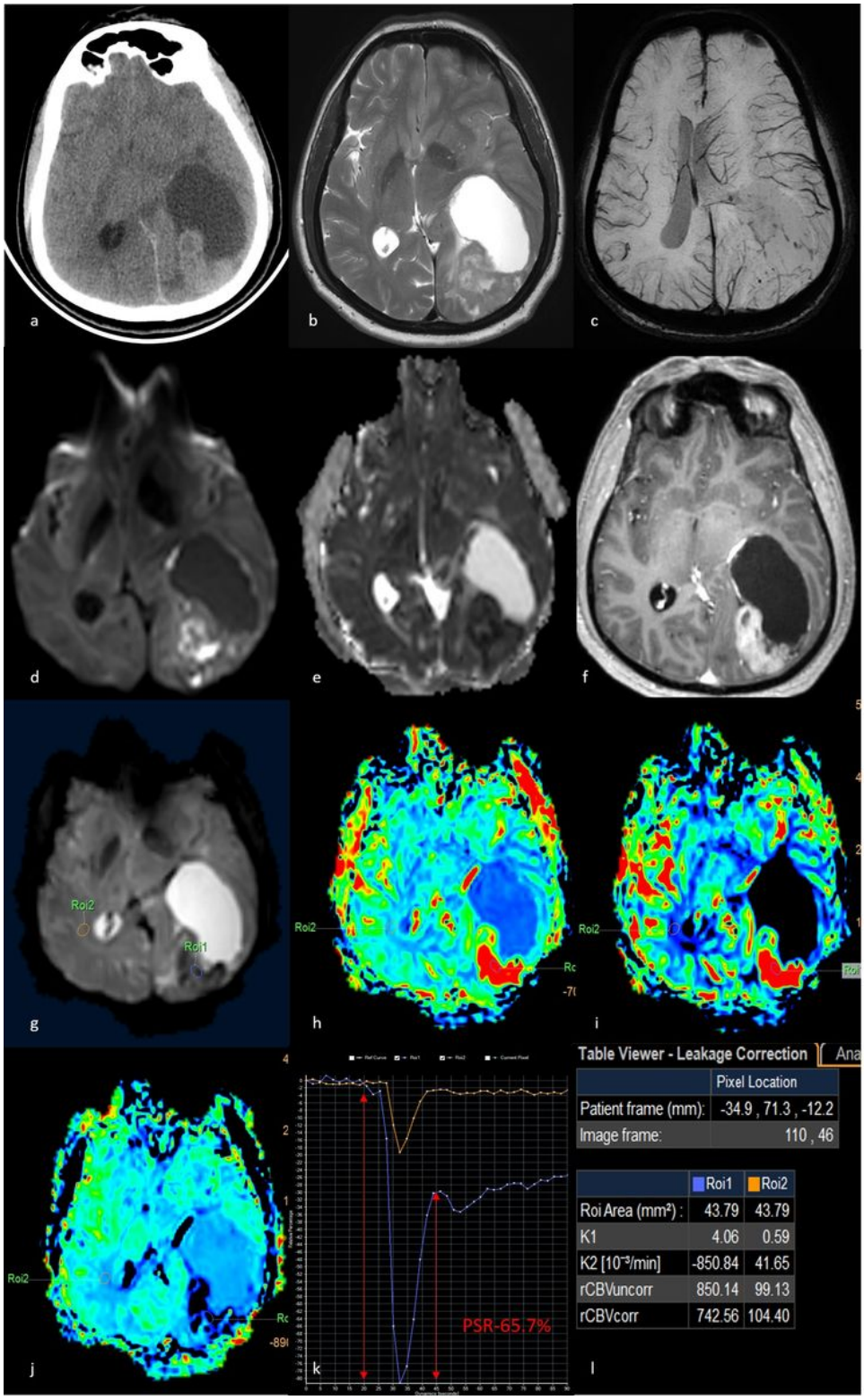

Figure 1

A 60year male known case of carcinoma left upper lobe presented with late onset of headache. CT (a) and conventional MRI (b-f) axial images show a solid cystic lesion in the left parietal region with minimal perilesional edema. The solid component is heterogeneously hyperdense on CT (a) and is iso-

hyperintense on T2Wimage (b) with subtle foci of blooming on SWI (c), partial restricted diffusion (d,e) and moderate post-contrast enhancement (f). DSC Perfusion (g) evaluated with the “Leakage correction” model is shown with corresponding multiparametric maps (h-j). rCBVuncor (h), rCBVcor (i), K2map(j), Time-signal intensity curve(k) and perfusion metrics (l) reveal a negative high K2 value and about 65.7% mean signal-intensity recovery. The lesion proved to be metastasis on histopathology.

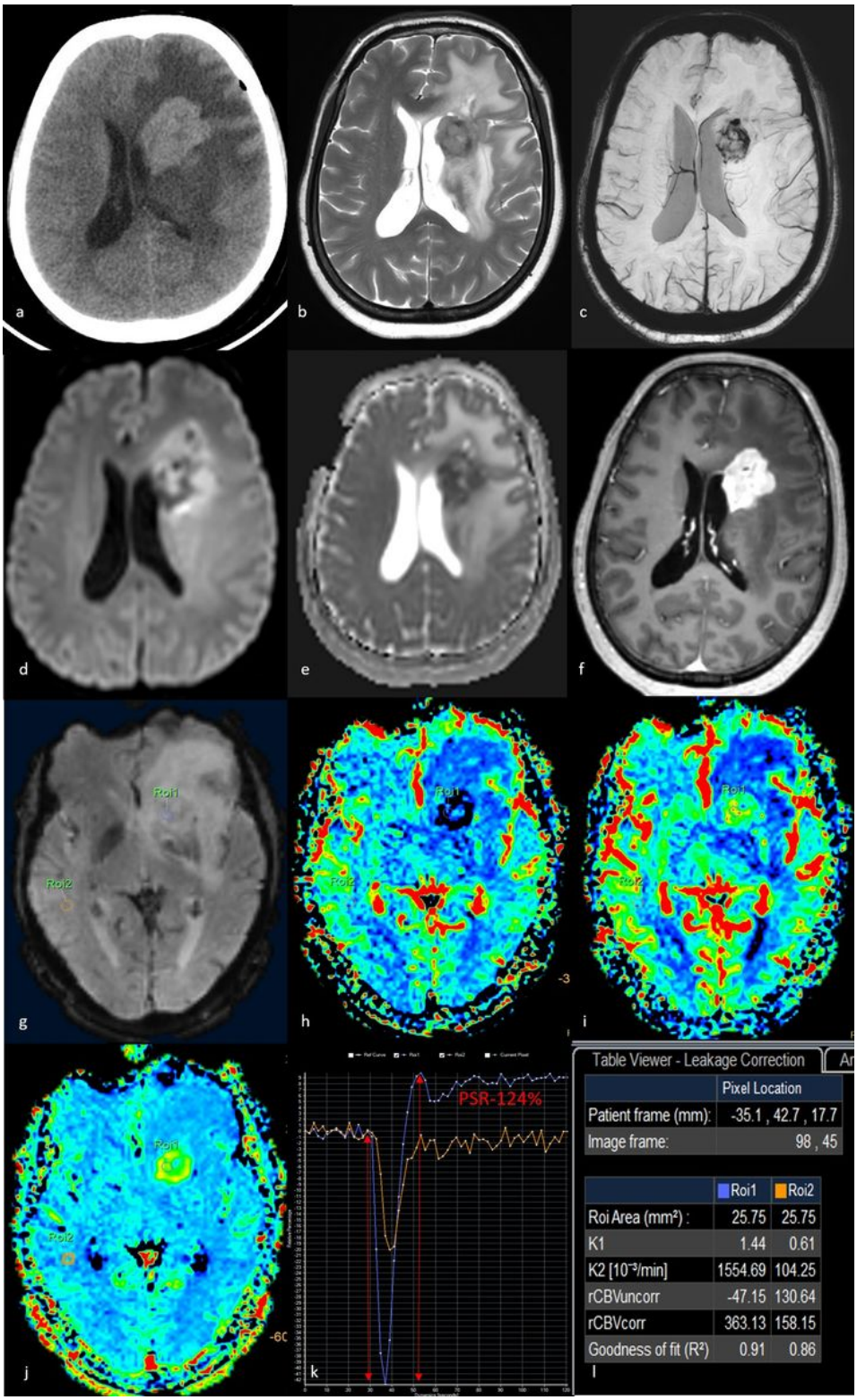

Figure 2

A 58year male with altered sensorium. CT (a) and conventional MRI (b-f) axial images show a solid lesion in the left anterior caudate adjoining the periventricular white matter in the left frontal lobe with moderate perilesional edema. The lesion is hyperdense on CT (a) and hyperintense on T2Wimage (b) with patchy areas of internal blooming on SWI (c), patchily restricted diffusion (d, e) and homogenous dense post-contrast enhancement (f). DSC Perfusion (g) evaluated with the “Leakage correction” model is shown with corresponding multiparametric maps (h-j). rCBVuncor (h), rCBVcor (i), K2map(j), Time-signal intensity curve (k) and perfusion metrics (l) reveal a positive high K2 value and about 124% mean signal-intensity recovery. Note the clear overshoot from the baseline. The lesion proved to be a B cell lymphoma on histopathology.

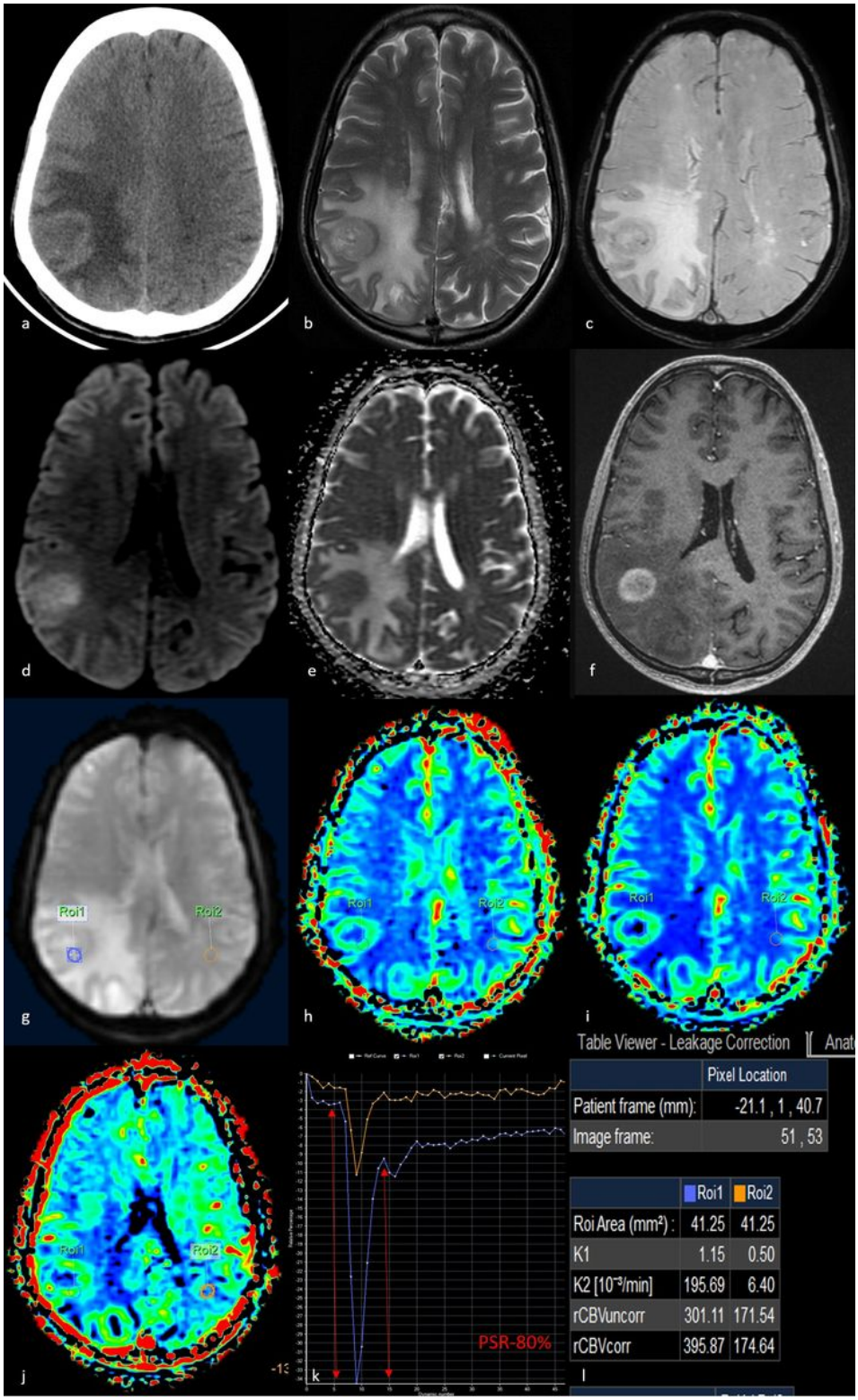

Figure 3

A 67year male with left hemiplegia. CT (a) and conventional MRI (b-f) axial images show a solid lesion in the right parietal region with moderate perilesional edema. The lesion is hyperdense on CT (a) and is hyperintense on T2Wimage (b) with subtle foci of blooming on SWI (c), mild homogeneous restriction of diffusion (d, e) and mild homogenous post-contrast enhancement (f). DSC Perfusion (g) evaluated with the “Leakage correction” model is shown with corresponding multiparametric maps (h-j). rCBVuncor (h),

rCBVcor (i), K2map(j), Time-signal intensity curve(k) and perfusion metrics (l) reveal a negative K2 value and about 80% mean signal-intensity recovery. The lesion proved to be a glioblastoma on histopathology.